XX IMEKO World Congress
Metrology for Green Growth
September 9–14, 2012, Busan, Republic of Korea

Experimental Investigation on DAC Glitch Measurement

S. Rapuano, E. Balestrieri, P. Daponte, L. De Vito

Dept. of Engineering, University of Sannio, Corso Garibaldi 107, 82100, Benevento, Italy
Ph.: +39 0824305817; Fax: +39 0824305840
E-mail: {rapuano, balestrieri, daponte, devito}@unisannio.it

Abstract - **The paper is aimed at experimentally analyzing the different DAC glitch definitions and measurement methods proposed in literature and adopted by manufacturers. Unfortunately, in fact, there is no universally accepted and unambiguous definition of a glitch. Therefore, the presented research work can give contributions and ideas for discussions focused to solve this problem and develop a new standard dealing with DAC terminology and test methods. An experimental analysis has been carried out and the obtained results have been critically analyzed to provide possible indications for the definition of a univocal and reproducible glitch measurement method.**

Keywords - glitch area; glitch energy; DAC test; reproducibility.

I. INTRODUCTION

Real-world analog signals such as temperature, pressure, sound, or images are routinely converted to a digital representation that can be more easily stored, processed, or transmitted. For these reasons, in the years, the scientific literature has been mainly focused on the Analog to Digital Converters (ADCs) issues [1,2,3,4]. However, in many systems, digital information must be converted back to the analog domain to carry out some real-world functions [5]. The components that perform this step are the Digital-to-Analog Converters (DACs). Their outputs are used to drive a variety of devices [5], like mobile phones or telecommunication, cordless communication networks, image processing and display systems, direct digital frequency synthesizers, signal reconstruction circuits, test equipment, high resolution imaging systems, and arbitrary waveform generators. Unfortunately, DAC operation is affected by non-idealities limiting the converter performance, as well as those of the system including it.

In particular, the high-speed high-accuracy DACs are sensitive to dynamic effects such as glitches. The DAC glitches, in fact, can limit the overall spectral performance of the converter and make it unusable for specific applications [6].

Glitch areas (amplitude*duration) have historically been huge and external glitch reduction circuitry has been necessary. Fortunately, modern DAC designs should not need active external glitch reduction circuitry [7]. However, the glitch area magnitude from one type of DAC to another can be several orders of magnitude apart [7]. To give some examples, the 12-bit AD664 datasheet reports a glitch area of 500 nVs, the 14-bit AD9764 a 1 nVs glitch area, the 16-bit AD768 a 35 pVs glitch area and the 14-bit DAC904 a 3pVs glitch area.

In any case, the DAC glitch response is critical especially for dynamic applications. For example, when the DAC is being used to reconstruct a waveform as a sinewave, any glitch on the output will degrade all the dynamic measures of that sinewave [7].

Therefore, glitch definition and measurement methods are essential both from the designers' and the users' points of view. Unfortunately, there is no universally accepted and unambiguous definition of a glitch [8]. This is a great problem since only unique and unambiguous DAC parameter definitions can avoid possible misinterpretations of the real device performance and make the right selection of a DAC for a specified application easy. Aware of this, the Waveform Measurement and Analysis Technical Committee (TC-10) of the IEEE Instrumentation and Measurement Society published a new standard on DAC terminology and test methods [9]. To give contributions and ideas for discussions that are related to the new IEEE DAC standard, a research project has been carried out to provide a unified approach to DAC terminology standardization [10-12]. In particular, glitch definition ambiguity and problems have been highlighted in [12].

The present paper presents an in-depth experimental analysis of glitch measurement procedures [12-18], starting from the results described in the previous work [12]. In particular, different glitch definitions and test methods have been compared by means of an experimental investigation focusing on (i) the applicability of each definition and test method; (ii) the required computational complexity; and (iii) the

possibility of automating the area/energy measurement procedure excluding the need of the operator supervision.

II. DAC GLITCH ISSUES

Ideally, when a DAC output changes it should move from one value to a new one monotonically. In practice, the output is likely to overshoot, undershoot, or both (Fig.1) [19]. This uncontrolled movement of the DAC output during a transition is known as glitch [19].

DAC glitches can arise from the following mechanisms: (i) capacitive coupling of digital transitions and clock signal to the analog output, and (ii) effects of some switches in the DAC, producing temporary spurious [13].

Capacitive coupling frequently produces roughly equal positive and negative spikes, which more or less disappear in the longer term. The glitch produced by switching time differences is generally unipolar, much larger, and of greater concern [13]. The glitch amplitude, in fact, can be as high as several least significant bit values (LSBs).

Glitches can be characterized by measuring the impulse area or energy from the midscale settling waveform. The midscale glitch, in fact, is usually considered to be the worst one, although a glitch can be present at whatever output value transition.

A comprehensive overview on DAC glitch definitions, taken from standards, scientific literature, and manufacturers' documentation, has been carried out in [12], highlighting existing similarities, ambiguities, and inadequacies. Then, DAC glitch, glitch area and energy definitions have been chosen, entirely adopted, if possible, or modified or completely rewritten considering that each parameter has to be unambiguously defined and practically measurable [12].

However, once found the unambiguous glitch parameter definitions, it is necessary to carry out the analysis of the test setup and the measurement methods by which these parameters can be evaluated. An extensive experimental comparison is also needed in order to highlight practical compatibility and reproducibility problems. Glitch definition and measurement methods, in fact, cannot be defined independently from each other. A good definition must be matched with a practically executable measurement method, able to avoid problems due to the lack of result reproducibility.

Glitch definition problems highlighted in [12] have been, therefore, experimentally analyzed to carry out an efficient, from the metrological point of view, measurement method.

Basically, the different approaches to the glitch definition can be related to the manufacturer sources. Since the different DAC design is often application-oriented, in fact, some glitch characteristics are marked more or less important according to the specific application. For example, in some datasheets the glitch area is used to characterize the impulses, in other datasheets instead the glitch energy is used. In the following, each aspect is treated separately.

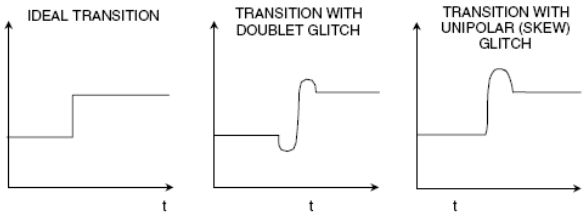

Figure 1. DAC Transitions (showing glitch) [19].

Measurement unit

A first problem comes from the measurement unit used for the glitch energy. Most of the existing definitions use volt seconds (picovolt or nanovolt) and not actual units of energy. This can be explained by the widespread habit of using the term glitch energy or impulse to refer to the area under the curve on a voltage-versus-time plot. However, clearly the term glitch energy must be considered a misleading name for indicating glitch area.

Integral approximation

The glitch area and energy are theoretically defined as time integrals, without using any approximation. However, for practical test reasons, the glitch area is often estimated as a sum of areas that are computed by an approximated waveform (triangular or square shape). The approximation method has a great influence on the results, as it will be clear in the following. However, not always this information can be found in the datasheets.

Impulse choice

Another problem arises from the disagree among the different manufacturers about what should be considered glitch in presence of oscillation transients. Some of them focus on the highest spike, others consider more oscillations. When considering the glitches due to data input changes, the secondary spikes are due to settlement effects that can compensate each other and are not the preeminent contributes, with the first spike being much bigger than the others. Even in such cases, usually, datasheets do not specify if the area under the negative-going spikes is subtracted from or is added to the area under the positive spikes to determine the glitch area and/or energy. As a result the glitch area and energy values are different, depending on these two cases. In the same way, the glitch area and energy values change when both the rising and falling edge glitches are considered.

Duration assessment

Another important consideration is whether taking or not into account error bands to define the spike durations. In the first case, of course, the error band width will influence the energy/area values. In the second case, the noise in the measurement system can affect heavily the energy/area measurement [12].

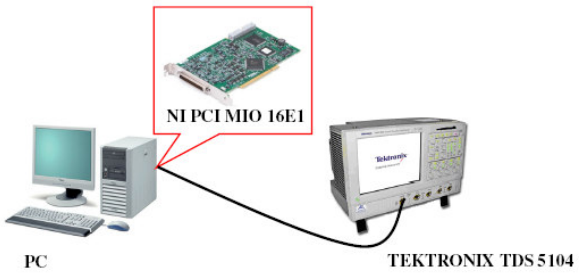

Figure 2. DAC glitch measurement test setup.

All the sketched degrees of freedom in specifying the glitch metrological characteristics can lead to incompatible measurements when different test technicians adopt different approaches without stating them. For such a reason, the research work presented in this paper is aimed at investigating experimentally the reproducibility of the results that can be achieved on the same devices, comparing the glitch measurement methods.

III. DAC GLITCH EXPERIMENTAL INVESTIGATION

The first objective of the work is the comparison of the different definitions and testing methods mostly currently used for the DAC glitch characterization in terms of glitch area. In particular, the reproducibility of the measurement results can be studied versus: (i) the area approximation methods, (ii) the impulse choice (inclusion or exclusion of the secondary spikes of the DAC output transient in the glitch computation; the addition or subtraction of positive and negative areas; the inclusion or not of both the rising and falling edge contributions), and (iii) the duration assessment (the error band amplitudes).

In the following, the experimental investigation carried out in the paper has been presented by firstly focusing on the test setup and waveform acquisition issues and, then, focusing on the objectives and considered hypothesis concerning the carried out data analysis.

III.A Test setup and waveform acquisition

In general, a wideband fast-settling oscilloscope is crucial to accurate glitch measurements. But even with modern DSOs and DPOs, overdrive should still be checked by changing the scope sensitivity by a known factor and being sure that all portions of the waveform change proportionally. Moreover, the sensitivity of the scope should be sufficient to measure the desired error band [12]. The results presented in the paper have been obtained from the test setup shown in Fig.2. In particular, the glitch values of the DAC embedded in the acquisition board NI PCI MIO 16E1, installed on and controlled by a PC, have been measured by means of the oscilloscope Tektronix TDS 5104. The midscale transition has been considered. A square wave with an amplitude of 5mV, corresponding to a LSB transition, and a frequency of 100 kHz, has been generated by the DAC with an update rate of 2.1 MHz. The glitch waveform has been acquired by the oscilloscope at a sample frequency of 5 Gsample/s, in records of 100000 points. Ten glitch waveform records have been acquired for each of six different oscilloscope acquisition settings, to analyze the effects of the instrument noise on the automatic procedure implemented to calculate the glitch value from the acquired waveforms. In particular, the first 10 glitch waveforms have been obtained by using a 32 sample averaging acquisition mode, and by limiting the input bandwidth to 20 MHz. The second group of glitch waveforms has been obtained using the same averaging conditions but a full oscilloscope bandwidth. The third group of glitch waveforms has been obtained by setting an 8 sample averaging, with a 20 MHz input bandwidth. The fourth group of glitch waveforms is the same of the third one but considering the full oscilloscope bandwidth. The fifth group of glitch waveforms has been acquired by applying the oscilloscope sample acquisition mode and considering an oscilloscope bandwidth of 20 MHz. Finally, the sixth group of glitch waveforms has been acquired by applying the oscilloscope sample acquisition mode and considering the full oscilloscope bandwidth.

III.B Data analysis

The experimental analysis and comparison have been carried out focusing on: (i) the applicability of each glitch definition and test method; (ii) the required computational complexity (depending on, for example, the number of samples to be acquired, the sample frequency, etc.); and (iii) the possibility of automating the area measurement procedure excluding the need of the operator supervision. These aspects are in fact essential to make the glitch measurement methods accessible to the ones who do not have sophisticated and expensive instrumentation and to be adopted in the industrial production environment.

The data analysis has been carried out considering for the glitch area calculation an error band of ± ½ LSB and the first peak area of the glitch waveform falling edge, since other spikes in measured glitch are missing.

In a first phase a square shape approximation has been applied to compute the glitch area for all the six measurement conditions described above. Glitch values have been carried out by means of a MatLab algorithm as follows:

1. the error band limits have been set as reference level ± ½ LSB (2.5 mV);
2. the glitch duration has been determined as the time interval going from the first waveform transition of the upper error band level with positive slope to the first waveform transition of the same level with negative slope;
3. the glitch amplitude has been determined as the difference between the peak waveform amplitude and the upper error band level;

4. the glitch area has been determined by simply multiplying the glitch amplitude and duration;
5. a reference level for the error band has been determined as the mean of the first 20000 points, making the presence of noise impossible to choose the reference value to add and subtract ½ LSB.

In a second phase different numerical integral approximations to compute the glitch area have been analyzed for all the six measurement conditions by decreasing the number of samples acquired. In particular, the rectangle methods (right and left corner, maximum and minimum corner and the midpoint), the trapezoid and Simpson's methods (Fig.3) have been considered [16,17]. The glitch area has been computed partitioning the glitch duration, that is the time interval determined by the glitch starting and ending instants, into N equal sub-intervals and applying the following formula:

$$A = \sum_{i=1}^{N} h_i w_i \tag{1}$$

where, w_i is the sub-interval width and h_i is the height, that is the glitch waveform amplitude at a specific time. The first value depends on the sampling period. The last value depends on the chosen numeric integral approximation method. In particular, the height value can be simply equal to the left, right, maximum or minimum side of the rectangle determined by the glitch sample at one of the i-partition extremes (right and left corner, maximum and minimum corner rectangle methods), as well as carried out by specific formulae (midpoint rectangle, trapezoidal and the Simpson's methods).
In the case of the midpoint rectangle method, the height is computed by the following formula:

$$h_i = \left[f\left(\frac{(x_i + x_{i+1})}{2} \right) \right] \tag{2}$$

Showing that the height value corresponds in this case to the glitch sample, $f((x_i+x_{i+1})/2)$, at the midpoint of the i-partition, calculated as the half sum of its first (x_i) and last (x_{i+1}) points.
For the trapezoidal and the Simpson's methods the applied height formulas are respectively:

$$h_i = \frac{1}{2}\left[f(x_i) + f(x_{i+1}) \right] \tag{3}$$

$$h_i = \frac{1}{6}\left[f(x_i) + 4f\left(\frac{(x_i + x_{i+1})}{2} \right) + f(x_{i+1}) \right] \tag{4}$$

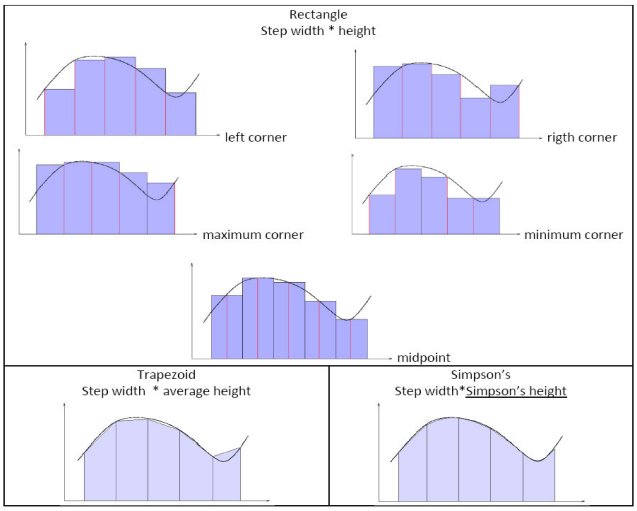

Fig. 3 Numeric integration methods.

In the trapezoidal case, the height value is the half sum of the glitch sample values $f(x_i)$ and $f(x_{i+1})$ at the first and last points of the i-sub-interval.
In the Simpson's method the sum, divided by 6, has 3 contributes: the glitch sample values at the start and end points of the sub-interval, $f(x_i)$ and $f(x_{i+1})$, and the glitch sample value corresponding to the midpoint of the same sub-interval, $f((x_i+x_{i+1})/2)$.
The number of samples has been decreased starting first considering a sampling step of 20 ps, secondly a step of 2ns, thirdly of 20 ns, then of 200 ns and finally of 400 ns. In these two last cases the numerical integration methods needing a nonlinear ($sinx/x$) interpolation to calculate the midpoint, that are the rectangle midpoint and the Simpson's methods, cannot be applied due to the unavailability of sample points (4 and 2 for the sample steps of 200 ns and 400 ns respectively).
The glitch values obtained by the numerical integration methods should be quite smaller than those achieved in the first phase by means of the square approximation being it a method to produce an over-approximation of the measured parameter.
The results have been provided by means of the estimated average glitch energy and its 95% confidence intervals according to the Student's t-distribution, because of the small number of acquired signals (ten) for each considered measurement condition (the same considered in the first phase).

IV. FIRST RESULTS OF THE EXPERIMENTAL COMPARISON

In Table 1 the results obtained in the first phase of the experimental analysis are shown, highlighting the maximum and the minimum glitch values of the 10 acquired records for each measurement condition. Looking at Table 1, it can be seen that the restriction of

the oscilloscope bandwidth greatly affects the computed glitch values. In these measurement conditions, in fact, the presence of the unfiltered noise can both increase the maximum amplitude reached by the acquired waveform and led to the wrong choice of the starting and/or final waveform points for determining the glitch duration. Consequently, the computation algorithm can provide higher values of glitch area.

Therefore, in case of noisy signals due to the test equipment neither the glitch measurement can be automated nor the error bandwidth can be fixed in a standard. In fact, in the case reported, the noise problem could be circumvented as the low-pass effects of the signal processing didn't affect the glitch waveform shape. In presence of different instrumentation, connections, environmental conditions, it could be impossible to filter out enough noise to adopt the ± ½ LSB error bandwidth without distorting the glitch. The elementary solution of requiring to set-up a measurement station whose noise level (to be defined and measured!) is well below half of the error bandwidth could limit significantly the adoption of the standard. An alternative solution could be the selection of an error bandwidth depending on the standard deviation of the overlapped noise. This could allow the automatic measurement of the glitch duration also in case of considerable instrumentation noise. Of course, the error bandwidth should always be specified in the datasheets. Another observation that can be done starting from this single group of results is that, in the manufacturer documents, when the error bandwidth is specified, the reference level is set to a conventional value (for example, the output corresponding to code 011111111111 or 100000000000). How this level is found experimentally is missing and should be specified.

The analysis results of the second phase have been focused on: (i) the differences among the results, expressed as means and confidence intervals, carried out by the single numerical integration method when the sampling step is increased; and (ii) the measurement compatibility of the results, expressed as means and confidence intervals, carried out by all the numerical integration methods at the same sampling step.

TABLE I. GLITCH MEASUREMENT RESULTS

Measurement Conditions	Max Glitch Area	Min Glitch area
Average acquisition mode (avg. 32); 20MHz bandwidth	18.4 nV s	17.9 nV s
Average acquisition mode (avg. 32); Full bandwidth	30.1 nV s	18.2 nV s
Average acquisition mode (avg. 8); 20MHz bandwidth	18.5 nV s	17.6 nV s
Average acquisition mode (avg. 8); Full bandwidth	33.5 nV s	18.4 nV s
Sample acquisition mode; 20MHz bandwidth	18.9 nV s	16.6 nV s
Sample acquisition mode; Full bandwidth	35.8 nV s	31.7 nV s

Considering the first target, the results have been similar for the six different measurement conditions, highlighting the right corner rectangle method to be the best one and the left corner rectangle method to be the worse one when the sampling step increases. In the first case, in fact, both the glitch mean values and the confidence intervals present smaller variation by increasing the sampling step than the other methods. The left corner rectangle method, instead, presents a greater decrease in the mean value when increasing the sampling step from 20 ns to 200 ns, and from 200 ns to 400 ns. Moreover, in some cases, as those shown in Fig. 4 for the sample acquisition mode both with 20MHz and full bandwidth, the confidence intervals at the last points have even about the same order of the mean values.

The analysis of the measurement compatibility among the results achieved by the seven numerical integration methods at the same sampling step has put in evidence the essential role of the 20 MHz filter to avoid the ambiguity in the detection of the starting and ending point of the glitch. In fact, as it can be seen in Fig. 5 for the case of the average acquisition mode on 8 waveforms, results carried out by all the numerical integration methods maintain compatibility both in the case of the 2ps and 2 ns sampling step when the filter is applied, otherwise the compatibility among all the methods is achieved only with the 2 ps sampling step.

Another important observation about the result compatibility analysis, independently from the particular measurement conditions, concerns the maximum and minimum corner rectangle methods, since they show to be more susceptible to the noise effects on the glitch starting and ending point detection, being the first to lose the compatibility with the other methods.

The average acquisition modes, both considering 8 and 32 waveforms, with and without the 20MHz filter, for the 200 ns sampling step, show lack of compatibility among the results carried out from the different numerical integration methods. In case of the 400 ns sampling step, instead, there is compatibility between two pair of methods, the right and maximum corner rectangle methods and the left and minimum corner rectangle methods, as shown in the Fig.5 for the average acquisition modes with 8 waveforms. As in those cases, only two samples have been considered in the computation, the pair compatibility can be explained with the coincidence of the minimum and the left points, and the maximum and the right points, considered to calculate the heigth in the integral computation.

In case of the sample acquisition mode, with and without the 20MHz filter, for the 200 ns and 400 ns sampling steps the larger confidence interval width of some numerical integration method result greatly influence their compatibility, as it can be seen in Fig. 5. The worse

cases are carried out with the two sample acquisition mode measurement conditions, having the biggest mean variability index, that in the case of 400 ns sampling step, for the left corner rectangle method reaches even the value of 110.8% and 82,9% (Fig.5), for the 20 MHz and the full bandwidth conditions, respectively.

Further observations can be done independently from the particular numerical integration method chosen, highlighting that in all considered cases better performance can be reached when the number of intervals to calculate the areas under the curve increases. It is also important to point out the strict relation between the particular shape of the curve to be integrated and the results produced by the particular numerical integration method.

Concerning the required time and processing power, instead, it can be observed that the rectangle methods evaluate the function once for each considered interval, whereas the trapezoid method evaluates it twice, and Simpson's method three times requiring more time and computations. Furthermore, the rectangle midpoint and the Simpson's methods require an interpolation to calculate the value of the curve at the midpoint of the considered intervals.

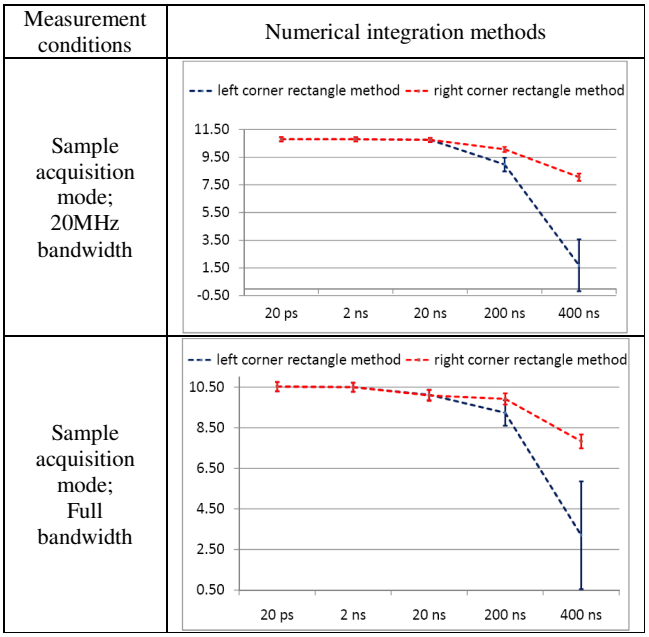

Fig. 4 Numerical integration methods at different sampling steps comparisons.

IV. CONCLUSIONS

High-speed high-accuracy DACs are particularly sensitive to dynamic effects such as glitches, that can limit the overall spectral performance of the converter and make it unusable for specific applications. Although some solutions to reduce the glitch have been successfully adopted in the years, DAC glitch response continue to be critical especially for dynamic applications. This together with the lack of a universally accepted and unambiguous glitch definition and test procedure can make arising misinterpretations of the real DAC performance and hard the right converter selection for a specified application.

The research work presented in this paper is aimed at investigating experimentally the reproducibility of the results that can be achieved on the DAC varying the definitions and the test methods focusing on (i) the applicability of each glitch definition and test method; (ii) the required computational complexity; and (iii) the possibility of automating the area measurement procedure excluding the need of the operator supervision.

First results of the conducted experimental investigation have shown that the restriction of the oscilloscope bandwidth greatly affects the computed glitch values. The presence of the unfiltered high frequency noise, in fact, can both increase the maximum amplitude reached by the acquired waveform and to led to the wrong choice of the starting and/or final waveform points for determining the glitch duration.

Therefore, in case of noisy signals due to the test equipment neither the glitch measurement can be automated nor the error bandwidth can be fixed in a standard. This can be more critical in all cases in which filtering out enough noise to adopt the ± ½ LSB error bandwidth without distorting the glitch is impossible. However, the selection of an error bandwidth depending on the standard deviation of the overlapped noise could allow the automatic measurement of the glitch duration also in case of considerable instrumentation noise.

The analysis of the numerical integration methods that can be applied to compute the glitch has highlighted once again the influence of the noise on the results. The methods more sensitive to this problem, as obtained from the experimental investigation, are the minimum and the maximum corner rectangle methods. Another interesting aspect concerns the number of samples and the sampling step considered. Increasing the sampling step, so reducing the number of samples available for the glitch computation, greatly affects the results, and this is a critical problem since in case of very small and fast glitch only few samples can be caught. The best numerical integration methods when decreasing the sampling points, as shown by the experimental results, is the right corner rectangle method, the worse being the left corner rectangle method. The analysis of the result compatibility among the different numerical integration methods has highlighted the considerable influence of the noise above all on the maximum and minimum corner rectangle methods. The worse results have been found when choosing the sample acquisition mode.

Future work will deal with the comparison of different definitions and testing procedures for DAC glitch by

means of an experimental investigation conducted on different converters. Successively, the glitch waveform dependence from the used measurement equipment will be investigated by changing the measurement instrument and the signal source used in the test.

REFERENCES

[1] T.E.Linnenbrink, J.Blair, S.Rapuano, P.Daponte, E.Balestrieri, L.De Vito, S.Max, S.J.Tilden, "ADC testing - Part 7 in a series of tutorials in instrumentation and measurements", IEEE Instrum. and Measurement Magazine, vol. 9, No. 2, April 2006, pp. 39-49.

[2] S.Rapuano, "Preliminary considerations on ADC standard harmonization", IEEE Trans. on Instrum. and Meas., vol.57, No.2, February 2008, pp.386-394.

[3] L.De Vito, S.Rapuano, D.Slepička, "ADC standard harmonization: Comparison of test methods - Phase II", IEEE Int. Intrum. and Meas. Tech. Conf., I²MTC 2009, pp. 1490-1495.

[4] L.De Vito, L.Michaeli, S.Rapuano, "An improved ADC-Error-correction scheme based on a bayesian approach", IEEE Trans. on Instrum. and Measurement, vol.57, No. 1, 2008, pp.128-133.

[5] D.G.Morrison, "Basics of design digital-to-analog converters", A Supplement to Electronic Design/November 10, 2003.

[6] J.Garcia, S.G.LaJeunesse, "Understanding glitch in a high speed D/A converter", Intersil technical brief, TB325.1, January 1995.

[7] L.Green, "ANALOG SEEKrets", Future Science Research Press, Pdf version, March 2011.

[8] K.Ola Andersson, M.Vesterbacka, "Modeling of glitches due to rise/fall asymmetry in current-steering digital-to-analog converters", IEEE Trans. on Circuits And Systems - I: Regular Papers, vol. 52, No. 11, November 2005.

[9] IEEE Std. 1658 "IEEE Standard for terminology and test methods for digital-to-analog converters", 2011.

[10] E.Balestrieri, S.Rapuano, "DAC consistent terminology: static parameter definitions", Measurement, vol.40, No.5, June 2007, pp.500-508.

[11] E.Balestrieri, S.Rapuano, "Defining DAC performance in the frequency domain", Measurement, vol.40, N.5, June 2007, pp.463-472.

[12] E.Balestrieri, "DAC time-domain specifications toward standardization", IEEE Trans. on Instrum. and Meas., vol.57, No.7, July 2008, pp.1290-1297.

[13] W.Kester, Ed., The data conversion handbook. Norwood, MA: Analog Device Inc., 2005.

[14] Philips, "Mixed signal testing cookbook", Nat. Lab. Rep. 7103, ver. 2.1, Oct. 1999.

[15] B.Jasper, Practical telecom DAC testing. [Online]. Available: www.testedgeinc.com

[16] J.Garcia, S.G.LaJeunesse, "Understanding glitch in a high speed D/A converter", Milpitas, CA: Intersil Corp., Jan. 1995. TB 325.1.[Online]. Available: www.intersil.com

[17] R.J.Van de Plassche, "CMOS integrated analog-to-digital and digital-to-analog converters", Boston, MA: Kluwer, 2003.

[18] Intersil, HI5721 datasheet. [Online]. Available: www.intersil.com

[19] J.Bryant, W.Kester, "Basics of ADCs and DACs, part 5", EETimes, Aug. 2007, [Online]. Available: http://www.eetimes.com

[20] S.Rosloniec, Fundamental Numerical Methods for Electrical Engineering, Springer, Chapter 5, 2008.

[21] G.B.Thomas, R.L.Finney, "Calculus and Analytic Geometry (9th ed.)", Addison Wesley, 1996.

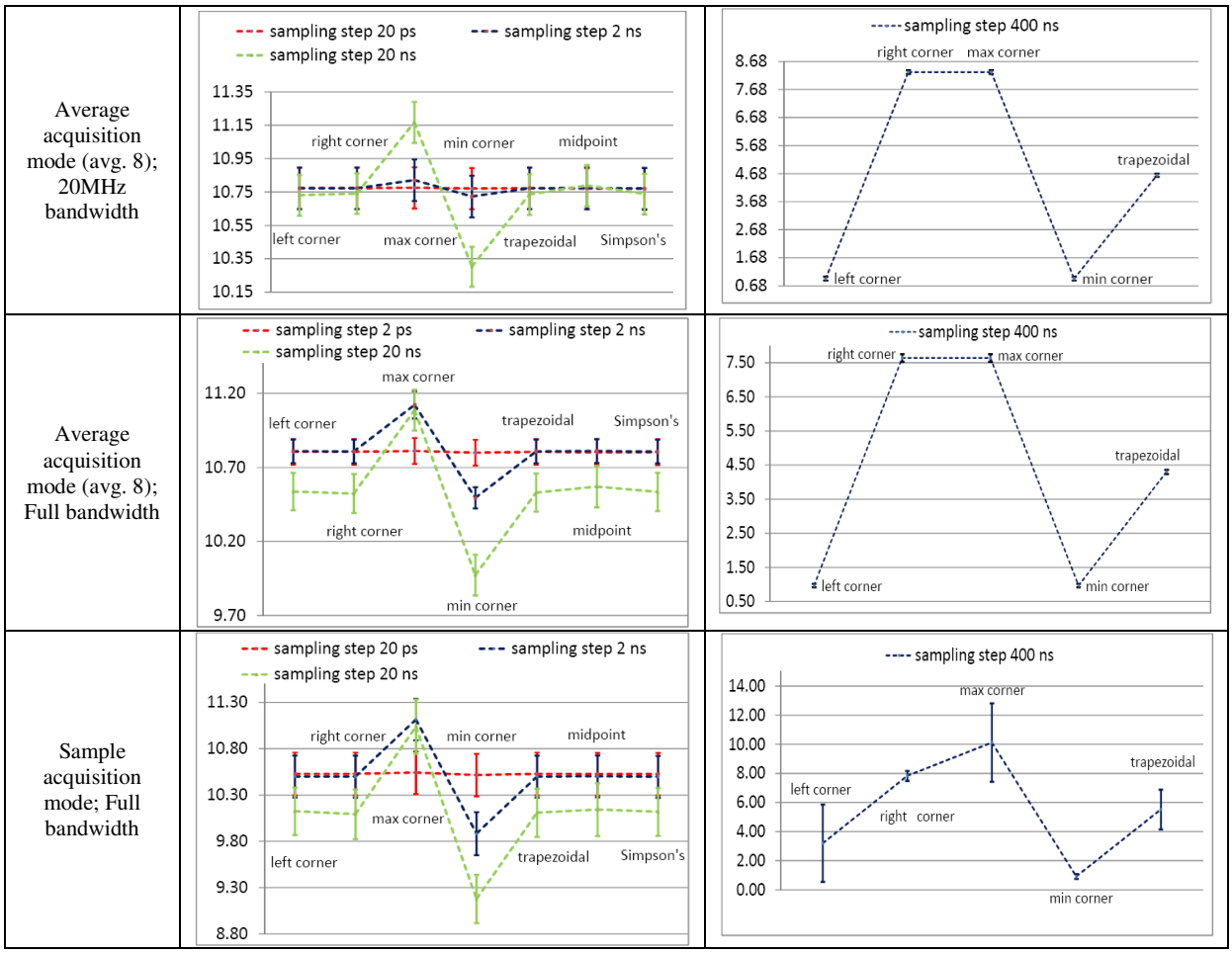

Fig. 5 Measurement compatibility of the numerical integration method results for increasing sampling steps.